Radiation resistance and mechanical properties of magnetron-sputtered Cr_2AlC thin films

Mohammed Imtyazuddin*, Anamul H. Mir , Matheus A. Tunes and Vladimir M. Vishnyakov

Institute for Materials Research, University of Huddersfield, Huddersfield, HD1 3DH, United Kingdom

Abstract

Cr_2AlC MAX phases were deposited using magnetron sputtering. The synthesis was performed via layer-by-layer deposition from elemental targets onto Si wafer and polished Inconel® 718 superalloy substrates at 650 K and 853 K. Transmission Electron Microscopy (TEM) characterisation showed that the thin films had a thickness of about 0.8 and 1.2 μm for Si and Inconel® substrates, respectively, and a MAX phase crystalline structure. Depositions onto Inconel substrate was performed in order to measure film mechanical properties. The films have hardness at around 15 GPa, reduced Young's modulus at around 260 GPa, do not delaminate and showed characteristic ductile behaviour during nanoscratching. Ion irradiations with *in situ* TEM were performed with 320 keV Xe^+ ions up to fluence 1×10^{16} ions·cm^{-2} at 300 K and 623 K. At 300 K the Cr_2AlC started to amorphise at around 0.3 dpa. At displacement levels above 3.3 dpa all crystalline structure was almost completely lost. Conversely, irradiations at 623 K showed no recordable amorphisation up to 90 dpa. It is discussed that the presence of many grain boundaries and low defect recombination energy barriers are responsible for high radiation hardness of Cr_2AlC MAX phase at 623 K. The thin film Cr_2AlC MAX phases have mechanical and radiation stability which makes them a candidate for fuel rod coating as Accident Tolerant Fuels (ATF) material for the next generation of nuclear reactors.

Keywords: Cr_2AlC; MAX Phases; ion irradiation; radiation damage; Accident Tolerant Fuels, thin solid films, Inconel® 718, hardness.

*) Corresponding author: Mohammed Imtyazuddin, U1771542@hud.ac.uk

Introduction

Currently, nuclear energy generation faces several challenges. After Fukushima-Daiichi Accident better protection of zirconium fuel assemblies is searched in the development of so named Accident Tolerant Fuel (ATF) solutions [1–3]. On the other side, it is expected that the materials which are designed for and to be used for the future fission reactors (e.g., Gen III+, IV), will undergo severe radiation damage (up to 100 displacements per atom) at high temperatures (573 -973 K). Very high dpa's can result in serious crystalline structural damage which will be detrimental to material's mechanical properties via precipitation, decomposition and amorphisation due to irradiation. New materials, such as high-entropy and refractory alloys [4] are under the scope of recent developments, but any innovative solution will have to be developed aiming at sustaining very high damage levels without adverse structural evolution. On the other hand, when the costs and natural availability of alloying elements are taken into consideration, their applicability within the nuclear materials niche will face additional challenges. As an alternative, thin solid films have been proposed as coating to nuclear fuel cladding alloys in order to increase its safety under normal and abnormal operational conditions.

So named $M_{n+1}AX_n$ (M: an early transition metal, A: group III or IV element and X: carbon or nitrogen) phases ($n \geq 1$) are nanolaminated ceramics with hexagonal crystal structure. The crystal structures are formed by layers of carbides or nitrides separated by layer of A atoms [5–7]. Attention in MAX phases have increased since their properties can be engineered to combine of both ceramic- and metal-like behaviours. The MAX phases are lightweight, machinable, have a high thermal and electrical conductivity. Some of them demonstrate high-temperature oxidation resistance and excellent thermal shock resistance [8–12]. It has been claimed that some MAX phases might be developed to have high radiation hardness [13–15]. Further investigations of MAX phase resistance to radiation is promising for usage in forthcoming fission reactor systems [16,17].

To date, the overall reported radiation hardness results for MAX phases are diverse [18–20] . Studies on Ti-based (A= Si, Al; X= C, N) bulk MAX phases exposed to neutron irradiation up to 0.1 dpa at 633 K and 968 K (high temperature) have shown some inconsistent resistance to damage accumulation. . Ti_3AlC_2 was observed to decompose to TiC. Ti_2AlN was seen to separate into TiN and Ti_4AlN_3 after irradiation at high temperature. However, in Ti_2AlC decomposition into TiC is not observed and Ti_3SiC_2 only displayed a small amount of lattice distortion [19]. In another study, Ti_2AlN_x/ (Ti, Al) N synthesised by dc magnetron sputtering were irradiated with 100 keV Ar^+ ion and showed resistance to amorphisation up to a fluence of 1.8×10^{15} ions/cm^2. It was suggested that the point defects created during the irradiation in this case were recovered due to the existence of nitrogen vacancies in the non-stoichiometric films [20].

Proton irradiation of Ti_3SiC_2 and Ti_3AlC_2 MAX phases performed up to 0.1 dpa at 623 K displayed significant dimensional instabilities by decomposition to their binary carbides [21]. Ti_2AlC phases were irradiated with He^+ at room and elevated temperatures. At room temperature, the sample showed microcracks due to changes in lattice parameters and accumulation of He. At all high temperatures, the samples showed no cracks. This stability was attributed to the high-effective recovery of defects [22]. Ti_3AlC_2 bulk samples were irradiated with He^+ up to a maximum of 5 dpa at 773 K. Expansion along the c-axis and shrinkage along the a-axis were observed, but, no amorphisation after irradiation was noticed [23].

MAX phases based on Zr are also thought to be prospective materials for the nuclear industry either in bulk form or as thin film coatings due to their low cross-section for thermal neutron absorption [24–27]. Lapauwa *et al.* synthesised Zr-based MAX phase by reactive hot pressing and found the Zr_2AlC MAX phase along with ZrC as a secondary phase. Vickers hardness of Zr_2AlC MAX phase was estimated to be at around 6.5 GPa. Horlait *et al.* sintered Zr-based MAX phases by partial substitution of M element by Mo, Ti and Cr. While the substitution of carbon by As or S was not successful. Partial substitution of A elements with Sb, Sn, and Pb shown to be promising. The amount of MAX phase in $Zr_2(Al_{0.5}Sn_{0.5})C$ and $Zr_2(Al_{0.5}Pb_{0.5})C$ was found to be 57 wt % and 65 wt %, respectively. However, amount of MAX phase in $Zr_2(Al_{0.5}Sb_{0.5})C$ was found to be lower than 30 wt %.

From all the previous works, it is believed that less radiation damage accumulation is observed when MAX phases are exposed to energetic particle irradiations at high temperatures. This allows to assume that irradiation defects produced in some MAX phases will probably self-heal (recombine) within the temperature range considered for future generation nuclear reactors [28].

Cr_2AlC MAX phase has a set of unique properties, even among the MAX phases. For instance, it has high-temperature oxidation resistance due to the presence of Al and Cr – both are high-density oxide formers [29,30]. The material demonstrates crack self-healing ability at elevated temperatures. This is based on aluminum oxide crack bridging due to high Al affinity towards oxygen and particularly high Al mobility in the phase as compared to metallic chromium alloys[31,32]. High oxidation resistance of Cr_2AlC [33] is combined with a relatively high hardness of around 14 GPa [34]. Cr_2AlC MAX phase thin films can be deposited at relatively low temperature by Physical Vapour Deposition techniques. The crystalline phase can be produced at the temperatures ranging from 723 to 858 K (depending on the type of sputtering targets used). Crystalline films can be obtained from amorphous compositions deposition followed by thermal annealing at above 873 K [35–38].

Until now, only limited to room temperature studies of the Cr containing MAX phases behavior under irradiation have been reported [39–42] . Ion-irradiation of Cr_2AlC and Cr_2GeC thin films with 320 keV Xe^{2+} ions up to 10^{13}–10^{14} ions/cm^2 at room temperature have led to full amorphisation. It is believed that the amorphisation takes place via a direct impact and defect accumulation in Cr_2GeC and Cr_2AlC respectively [42]. Also, for comparison, V_2AlC and Cr_2AlC bulk samples have been irradiated with 1 MeV Au^+ ions over a series of fluences varying from 1.9×10^{14} to 1.9×10^{16} ions/cm^2 at room temperature. XRD and TEM data showed that irradiated V_2AlC retained crystallinity, but, a phase conversion from HCP to FCC lattice structure has occurred. On the other hand, Cr_2AlC was transformed to γ-Cr_2AlC at 1.0×10^{14} ions/cm^2 and amorphised at 1.0×10^{16} ions/cm^2 [41].

In this present work, Cr_2AlC thin films were irradiated with 320 keV Xe^+ ions at room (300 K) and elevated (623 K) temperatures. This allowed to follow microstructural evolution at different fluences and demonstrated the material amorphisation at 300 K and stability of Cr_2AlC at 623 K towards ion damage.

Materials and Experimental techniques

Magnetrons sputtering deposition from elemental Cr, Al, and C targets was used. The samples were deposited on Si (100) and Inconel® 718 superalloy substrates at 650 K and 853 K correspondingly. The substrate heating was performed from the backside of the substrate. The temperature is measured on the heater. This means that the deposited surface will have rather lower temperature. Silicon had thickness of 400 microns whilst Inconel was 3000 microns thick. This potentially produces requirement for higher temperature on the heater in order to

promote crystallisation of MAX phases on the Inconel substrate. A full description of this deposition system can be found elsewhere[43]. After deposition, the thin film thicknesses was at around 0.8 μm for Si and 1.2 μm for the Inconel substrates.

The specimens for in-situ TEM ion irradiation were prepared by conventional focused ion beam milling using 30 keV Ga ions. The same system was used for milling and polishing. The material was protected from Ga implantation damage by a deposition of 3.5 microns platinum layer prior to milling. Ion irradiations with 320 keV Xe^{+} were performed at 300 K and at 623 K using MIAMI-2 TEM with in-situ ion irradiation facility at the University of Huddersfield [44]. The dpa levels shown in Fig.1 were calculated using SRIM 2013 assuming a sample thickness of about 150 nm, average atomic density of 8.85 $\times 10^{22}$ atoms/cm^3 and displacement energies of 40eV for Cr, Al, and C [45]. The maximum fluences were 1.68 $\times 10^{15}$ ions/cm^2 and 2.1x 10^{16} for 300 K and 623 K correspondingly. It is possible to use SRIM2013 built-in table data for atom displacement. In this case, we would have displacement energies of 25, 25 and 28 eV. This leads to the rise of calculated damage by almost 60 %, as shown in Fig.1. We have used uniform 40 eV energy for reporting in this paper.

The Cr_2AlC thin film microstructures were characterised by using bright-field TEM (BFTEM) and selected-area diffraction pattern (SAED) and X-Ray Diffraction. Crystallographic indexing of the crystalline structure of the Cr_2AlC thin films was performed using data reported previously in the scientific literature[36,38,46].

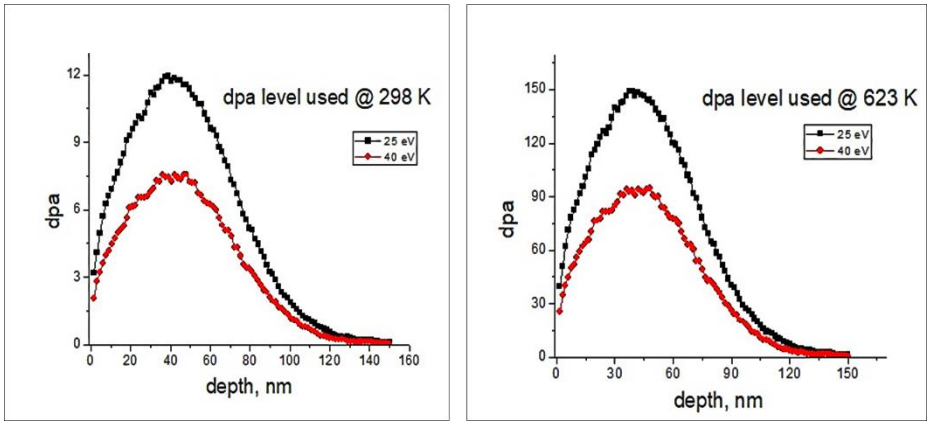

Fig .1 Variation in dpa levels due to Ed (displacement energy) reported by others[40,41] and in present work Ed=40eV[45], at fluence of 1.68 $\times 10^{15}$ ions/cm^2 and 2.1$\times 10^{16}$ for 300 K and 623 K

In order to assess the mechanical properties of the deposited coatings, a Micro Materials NanoTest platform was used. The indentations were performed to different depth to separate film properties from the substrate effects. Nanoscratching was done with an old (blunt for nanoindentation) Berkovich tip with ramping load from zero up to 500 mN over 500 micrometre trace. The scratch traces were inspected in Scanning Electron Microscope (SEM).

Results:

Fig.2, displays the material EDX spectrum. Major chromium L-lines around 500 eV are clearly separated. Oxygen K-line, if present in the material in sufficient quantity, usually placed in between Cr lines makes one unquantifiable line at this energy interwal. As the Cr lines are clearly separated, we can presume that the oxygen content is below 5 at%. We do not observe any additional X-ray signals in the spectra and presume that the material is pure. The chemical composition was quantified from the EDX spectra with ZAF corrections. We would assumethat the error in quantification is within 5%. We have obtained quite similar result for the material

quantification by an independent EDX analysis in TEM. The composition within the error confirms to stoichiometry of Cr_2AlC MAX phase.

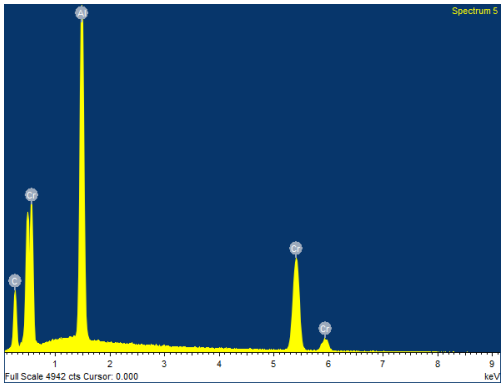

Elements	Concentration, atomic %
Cr	**53.40**
Al	**22.76**
C	**23.84**

Fig.2. EDX spectrum and quantification of the results. Quantification error within 5%.

The microstructural evolution of the Cr_2AlC thin films during heavy ion irradiation with 320 keV Xe ions at 300 K is presented in the set of figures 3(a-d), which comprises BFTEM and SAED micrographs. At this irradiation temperature, partial amorphisation of the thin film initial crystal structure was observed to occur at doses of around 0.3 dpa as shown in figure 3(b). The amorphisation phenomenon was evident by monitoring the diffraction pattern *in situ* in the TEM. The central diffuse amorphous ring was evidenced even at 0.3 dpa.

Fig 3b taken at 0.3 dpa demonstrates that the material partially becomes amorphous and partially alters structure. There is not enough data at the moment to identify the emerging phase. The new structure can be one of earlier reported γ-Cr_2AlC HCP phase, indexed for 002, 102, and 110 planes. However, we do not have enough data at the moment to confirm or reject the existence of γ-Cr_2AlC in our case. Loss of high intensity crystalline reflections from Cr_2AlC planes can be also observed. Fig 3d shows amorphous rings with very weak crystal diffraction spots at 3.3 dpa contributed by the unirradiated part of specimen present beyond the ion range. To confirm this, the specimen was taken out of the TEM, turned around and then irradiated from the backside to a combined fluence of 1.68×10^{15} ions/cm^2 at which complete amorphization was observed (this data is not shown here).

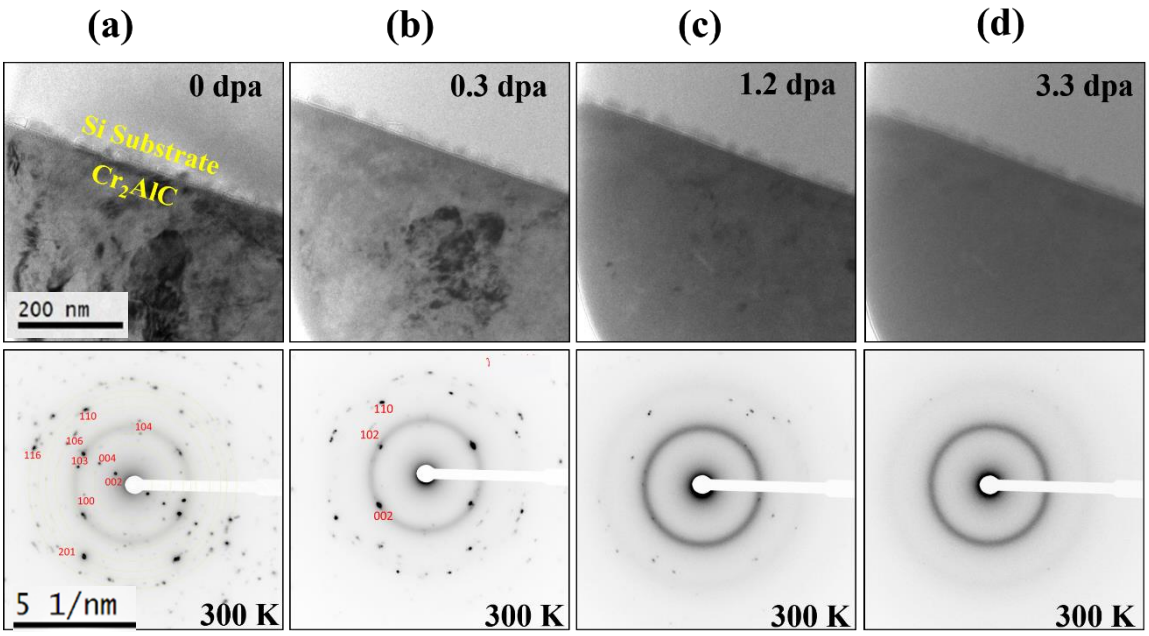

Fig. 3: *In situ* microstructural evolution of the Cr_2AlC thin film under 320 keV Xe irradiation at 300 K.

The microstructural evolution of the heavy ion irradiated Cr_2AlC thin films at 623 K is shown in the set of BFTEM and SAED micrographs on figures 4(a-d). As opposed to the irradiations at 300 K, amorphisation was not observed to occur at any doses. This clearly can be established by the absence of diffuse amorphous diffraction rings. At the end of the irradiations at a dose of 90 dpa (or 2.1×10^{16} ions·cm^{-2}), new phase creation, e.g. phase transformation, was also not evident.

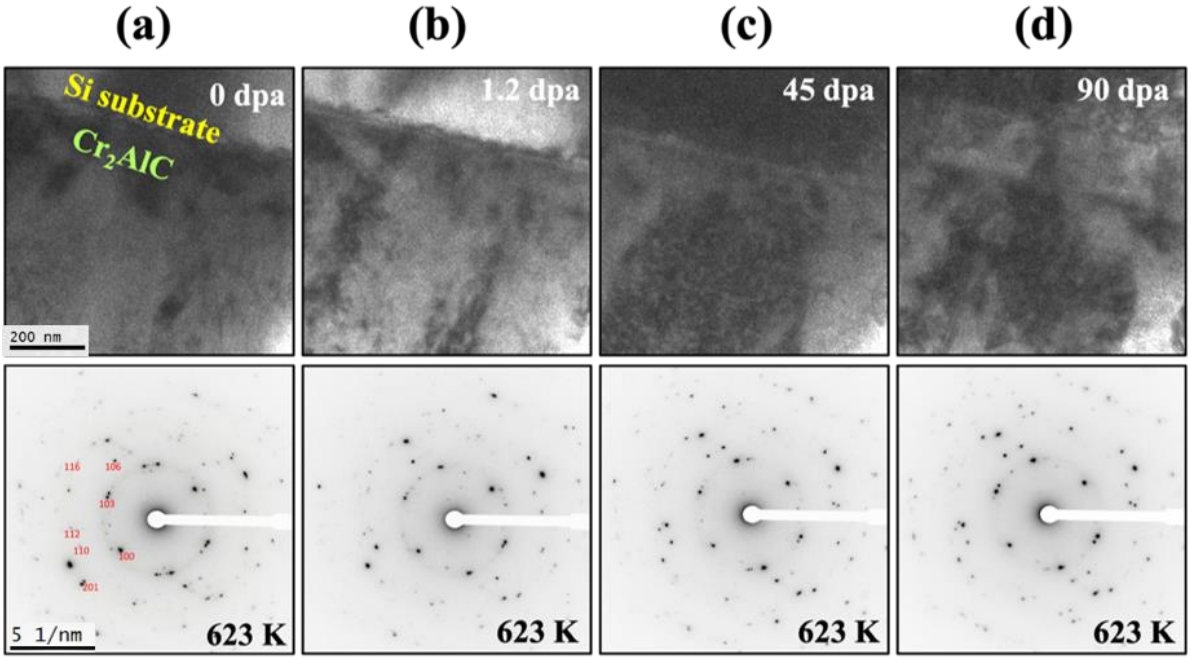

Fig. 4. In situ microstructural evolution of the Cr_2AlC thin film under 320 keV Xe irradiation at 623 K.

The results for the film mechanical properties testing are presented on Fig. 5. Hardness and Reduced Young's modulus depend on indentation depth (plastic depth). This is due to the fact that the superalloy has a lower hardness and Young's modulus than the film (hardness at around 3.7 GPa and Young's modulus at around 200 GPa). As indentation load and corresponding indentation depth increase, the measured parameters switch from the film parameters to the mixed, film-substrate, values. It is well understood that the plastic interaction zone extends to about 3 times the plastic penetration depth during nano and microindentation [47]. Therefore, for a film thickness of about 800 nm, the film properties are represented by plastic penetration depths of less than 270 nm. In the present case, the approximately depth for the visible transition was at around 250 nm. Bearing this in mind, the film parameters were averaged up to a depth of 227 nm. The hardness and Reduced Young's modulus of the film were found to be 15 ± 1.8 GPa and 259 ± 20 GPa. Big standard deviations are due to the film nature which causes slip-ins, as observed before by many authors. Nanoscratching showed "metal-like" plastic behaviour of the film and absence of any delamination under scratching conditions. Also, no cracks in the film around the scratches were observed (Fig 5(b)).

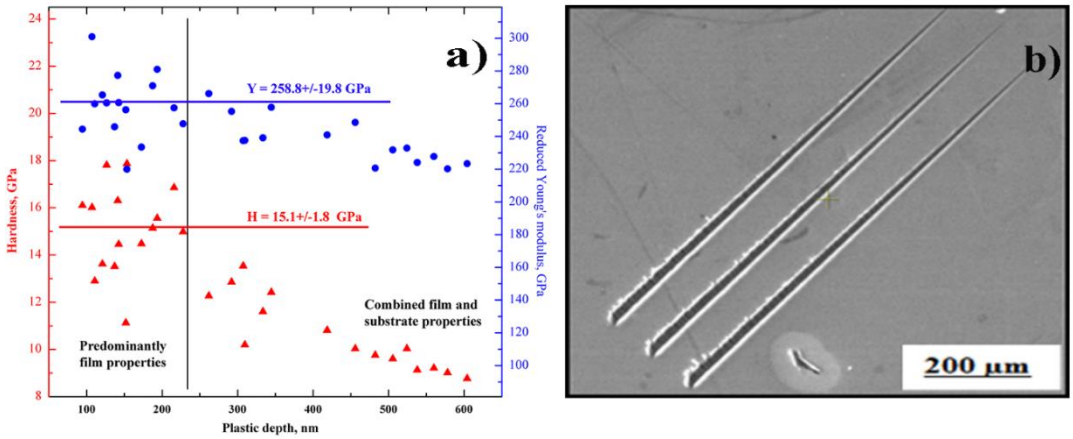

Fig. 5: Nanomechanical testing of Cr_2AlC thin films on Inconel® 718 superalloy. (a) Hardness and Reduced Young's modulus and (b) SEM surface image after nanoscratching.

Discussion

Irradiations done at 300 K showed amorphisation and some phase transformation. The observable amorphisation indicates that significant parts of the initial crystalline lattice lose crystallinity. Taking into the account that we have amorphisation and phase transformation, we can assume that the primary process is amorphisation and this occurs when a large number of atoms in the cascade get displaced and then do not return to the initial crystalline positions. It is known that amorphous Cr_2AlC composition can be crystallised at temperatures above 873 K and the room temperature is not enough to re-crystallise the amorphous phase [46]. As the re-crystallisation during irradiation happens into an intermediate phase it is most likely that full re-crystallisation to MAX phase is point defect diffusion limited, see below. In this case the defective amorphous phase partially collapses into possible γ-Cr_2AlC HCP phase during cascade quenching. This is happening as not all vacancies are filled with displaced atoms and the MAX phase is not restored but potentially γ - Cr_2AlC is created. This process of transition from MAX phase into γ-Cr_2AlC was noticed in previous studies during ion irradiations. Cabioc'h.*et al.* found decomposition of Cr_2AlC MAX phase irradiated by 320 keV Xe ion with a fluence range of 10^{15} ions/cm^2 at room temperature into γ - Cr_2AlC[42] . Chenxu *et al*, also found the γ - Cr_2AlC formation when the sample was irradiated with 1 MeV Au^+ ions at room temperature[41].

As at higher fluences the material is fully amorphised we need to assume that at room temperature predominantly amorphous phase remains with only partial creation of γ - Cr_2AlC. Over the fluence increase this leads to full material amorphisation at room temperature irradiations.

Historically, the formation of γ-Cr_2AlC was reported during the synthesis of Cr_2AlC thin films at different temperatures. Shtansky *et al.* identified γ-Cr_2AlC during film deposition from a Cr_2AlC compound target on to a substrate at 300 °C. The films with γ-Cr_2AlC were annealed at 800 °C to form Cr_2AlC along with Cr_7C_3 and Cr_3C_2 secondary phases [48]. In another study by Abdulkadhim *et.al* it was found that γ-Cr_2AlC phase is an intermediate state during crystallisation of Cr_2AlC at the temperature range of 843 to 883 K from an amorphous Cr_2AlC thin film [46]. From these observations, it is believed the establishment of γ-Cr_2AlC phase during crystallisation is diffusion controlled.

Jingren Xiao *et al* [49] evaluated the resistance to radiation of various MAX phases based on first-principle simulations. It was found the weaker bonding of M–A in Cr_2AlC MAX phase is performing similar to ionic bond which permits to re-establish the damaged structure to coherent crystalline lattice more easily. In addition, the bonding of A–X, AlC in our case, is not as strong as in other carbides. This means that intermediate phases are not very stable and Cr_2AlC MAX has enhanced self-healing ability [32,45].

On the other hand, for irradiations done at 623 K, the MAX phase thin film remains crystalline with no visible amorphisation. Furthermore, there was no conversion to anything resembling γ-Cr_2AlC, the MAX phase seems to be unperturbed by the irradiation. This stability can be attributed to the high recovery rate of thin film Cr_2AlC MAX phase at 623 K. Following the above logic we need to assume that at 623 K and possible continuous defects mobility coursed by irradiation we have shift of balance between amount of amorphisation and amount of defected phases (like possible γ-Cr_2AlC) towards the crystalline phases, which, due to the defect diffusion, is sufficient to recombine interstitials and vacancies and maintain initial crystallinity.

In principle, this MAX phase behaviour under irradiation at elevated temperature is in good agreement with previously published research on irradiation of MAX phases. Huang *et al*, for instance, found high recovery rate of defects in Ti_3SiC_2 and Ti_3AlC_2 irradiated with 7 MeV Xe^{26+} ion at 600 °C [50].

The behaviour is also can be well understood from the general principle of defect creation, migration, clustering and annealing. Material exposure to energetic particles leads to the creation of point defects on the first instance. While computational models describe energies for carbon vacancies and antisite formation, there is no data on barriers for defect recombination [40]. Recombination can be not so effective if there are energy barriers to recombination, high defect mobility, deep energy traps for the defects and/or defect clustering is thermodynamically beneficial at the irradiation temperature. Migration of defects might lead to clustering by coalescence and this, after a while resulting in loss of crystallinity [51,52]. Nanocrystallinity, as in our case, thought to limit mobility of migrating defects [53,54]. Grain boundaries can act as deep level defect sinks. Trapping defects on grain boundaries is well known and, for instance, recent studies on radiation stability of different nanocrystalline materials shown high radiation resistance due to the formation of denuded and dislocation denuded zones at room temperature and high temperatures [55–58]. Nanocrystallinity, while providing abundance of grain boundaries, might also create shallow defect sinks. Shallow sinks will keep high concentration of "free" to migrate in the lattice defects and lead, in the absence of clustering, to the effective defect recombination and the MAX phase restoration, self-healing. We propose that nanocrystallinity of the Cr_2AlC MAX phase provides additional and effective structure for exceptionally high radiation hardness at 623K.

Recently the bonding between bulk Cr_2AlC MAX phase and Inconel 718 at high temperature (1273 K) was studied [33]. Good bonding with some Al diffusion into Inconel was observed. In our case well adhered Cr_2AlC MAX film on Inconel 718 was created. The deposition temperature is too low to provide any diffusion bonding, however good adhesion is established at the easily achievable industrial deposition conditions.

Conclusions

The radiation resistance of Cr_2AlC thin films, irradiated by 320 keV Xe ions up to maximum fluences of 7.4×10^{14} and 2.1×10^{16} ions/ cm^2 at 300 K and 623 K (350 ºC) were investigated using heavy ion irradiation *in situ* within a TEM. The Cr_2AlC thin films were

irradiated at 300 K and partially amorphised (possibly after decomposing into γ-Cr_2AlC structure) at 0.3 dpa. At 3.3 dpa (7.4x 10^{14} ions/ cm^2), the Cr_2AlC thin films amorphises with some weak spots still observable in the diffraction patterns.

However, the Cr_2AlC MAX phase thin films, irradiated at 623 K (350 ºC) remains crystalline without visible amorphous phase formation up to very high damage level, which exceeds 100 dpa. Moreover, at 90 dpa (2.1x 10^{16} ions/ cm^2), the Cr_2AlC thin films remain crystalline without any decomposition. The resistance to amorphization at 623 K temperature is believed to be due to the efficient recovery of defects in the nanocrystalline grains and shallow sinks at the nanocrystalline grain boundaries. Nanoscratching shows good adhesion to Inconel 718 substrate, absence of delamination and "metallic" behaviour without film cracking. In combination with good adhesion to Inconel, high mechanical and radiation hardness makes Cr_2AlC MAX phase thin films good candidate for use in, high temperature and radiation, environments.

The exact mechanisms of radiation damage and especially healing processes are not clear, particularly at a moderate temperature such as the results herein present at 623 K, further works are needed in order to shed light on the radiation tolerance mechanisms of Cr_2AlC phases.

Acknowledgement

Mohammed Imtyazuddin, a PhD student, acknowledges some training and travel support by Il Trovatore, an EU project 740415.

References

[1] T. Cheng, J.R. Keiser, M.P. Brady, K.A. Terrani, B.A. Pint, J. Nucl. Mater. 427 (2012) 396–400.

[2] K.A. Terrani, J. Nucl. Mater. 501 (2018) 13–30.

[3] M.A. Tunes, F.C. da Silva, O. Camara, C.G. Schön, J.C. Sagás, L.C. Fontana, S.E. Donnelly, G. Greaves, P.D. Edmondson, J. Nucl. Mater. 512 (2018) 239–245.

[4] M.A. Tunes, V.M. Vishnyakov, Mater. Des. 170 (2019) 107692.

[5] D.J. Tallman, L. He, B.L. Garcia-Diaz, E.N. Hoffman, G. Kohse, R.L. Sindelar, M.W. Barsoum, J. Nucl. Mater. 468 (2016) 194–206.

[6] S.H. Shah, P.D. Bristowe, Sci. Rep. 7 (2017) 9667.

[7] D.W. Clark, S.J. Zinkle, M.K. Patel, C.M. Parish, Acta Mater. 105 (2016) 130–146.

[8] M.W. Barsoum, Prog. Solid State Chem. 28 (2000) 201–281.

[9] P. Eklund, M. Beckers, U. Jansson, H. Högberg, L. Hultman, Thin Solid Films 518 (2010) 1851–1878.

[10] M.W. Barsoum, T. El-Raghy, J. Am. Ceram. Soc. 79 (1996) 1953–1956.

[11] J.D. Hettinger, S.E. Lofland, P. Finkel, T. Meehan, J. Palma, K. Harrell, S. Gupta, A. Ganguly, T. El-Raghy, M.W. Barsoum, Phys. Rev. B 72 (2005) 115120.

[12] D. Music, J.M. Schneider, JOM 59 (2007) 60–64.

[13] N. V Tzenov, M.W. Barsoum, J. Am. Ceram. Soc. 83 (2000) 825–832.

[14] T. El-Raghy, A. Zavaliangos, M.W. Barsoum, S.R. Kalidindi, J. Am. Ceram. Soc. 80 (1997) 513–516.

[15] Z. Sun, Y. Zhou, M. Li, Acta Mater. 49 (2001) 4347–4353.

[16] P. Yvon, F. Carré, J. Nucl. Mater. 385 (2009) 217–222.

[17] E.N. Hoffman, D.W. Vinson, R.L. Sindelar, D.J. Tallman, G. Kohse, M.W. Barsoum, Nucl. Eng. Des. 244 (2012) 17–24.

[18] M.A. Tunes, R.W. Harrison, S.E. Donnelly, P.D. Edmondson, Acta Mater. 169 (2019) 237–247.

[19] D.J. Tallman, E.N. Hoffman, E.N. Caspi, B.L. Garcia-Diaz, G. Kohse, R.L. Sindelar, M.W. Barsoum, Acta Mater. 85 (2015) 132–143.

[20] J. Ward, S. Middleburgh, M. Topping, A. Garner, D. Stewart, M.W. Barsoum, M. Preuss, P. Frankel, J. Nucl. Mater. 502 (2018) 220–227.

[21] R. Su, H. Zhang, L. Shi, H. Wen, J. Eur. Ceram. Soc. 39 (2019) 1993–2002.

[22] M. Bugnet, T. Cabioc'h, V. Mauchamp, P. Guérin, M. Marteau, M. Jaouen, J. Mater. Sci. 45 (2010) 5547–5552.

[23] M.K. Patel, D.J. Tallman, J.A. Valdez, J. Aguiar, O. Anderoglu, M. Tang, J. Griggs, E. Fu, Y. Wang, M.W. Barsoum, Scr. Mater. 77 (2014) 1–4.

[24] T. Lapauw, K. Lambrinou, T. Cabioc'h, J. Halim, J. Lu, A. Pesach, O. Rivin, O. Ozeri, E.N. Caspi, L. Hultman, P. Eklund, J. Rosén, M.W. Barsoum, J. Vleugels, J. Eur. Ceram. Soc. 36 (2016) 1847–1853.

[25] E. Zapata-Solvas, S.-R.G. Christopoulos, N. Ni, D.C. Parfitt, D. Horlait, M.E. Fitzpatrick, A. Chroneos, W.E. Lee, J. Am. Ceram. Soc. 100 (2017) 1377–1387.

[26] D. Horlait, S. Grasso, A. Chroneos, W.E. Lee, Mater. Res. Lett. 4 (2016) 137–144.

[27] D. Horlait, S.C. Middleburgh, A. Chroneos, W.E. Lee, Sci. Rep. 6 (2016) 18829.

[28] J.C. Nappé, I. Monnet, P. Grosseau, F. Audubert, B. Guilhot, M. Beauvy, M. Benabdesselam, L. Thomé, J. Nucl. Mater. 409 (2011) 53–61.

[29] Z.J. Lin, M.S. Li, J.Y. Wang, Y.C. Zhou, Acta Mater. 55 (2007) 6182–6191.

[30] Z. Lin, Y. Zhou, M. Li, J. Wang, Zeitschrift Für Met. 96 (2005) 291–296.

[31] S. Li, L. Xiao, G. Song, X. Wu, W.G. Sloof, S. van der Zwaag, J. Am. Ceram. Soc. 96 (2013) 892–899.

[32] R. Pei, S.A. McDonald, L. Shen, S. van der Zwaag, W.G. Sloof, P.J. Withers, P.M. Mummery, J. Eur. Ceram. Soc. 37 (2017) 441–450.

[33] M. Sokol, J. Yang, H. Keshavan, M.W. Barsoum, J. Eur. Ceram. Soc. 39 (2019) 878–882.

[34] J.M. Schneider, D.P. Sigumonrong, D. Music, C. Walter, J. Emmerlich, R. Iskandar, J. Mayer, Scr. Mater. 57 (2007) 1137–1140.

[35] Y. Li, G. Zhao, Y. Qian, J. Xu, M. Li, J. Mater. Sci. Technol. 34 (2018) 466–471.

[36] C. Walter, D.P. Sigumonrong, T. El-Raghy, J.M. Schneider, Thin Solid Films 515 (2006) 389–393.

[37] V. Vishnyakov, O. Crisan, P. Dobrosz, J.S. Colligon, Vacuum 100 (2014) 61–65.

[38] J.M. Schneider, Z. Sun, R. Mertens, F. Uestel, R. Ahuja, Solid State Commun. 130 (2004) 445–449.

[39] C. Wang, Z. Han, R. Su, J. Gao, L. Shi, Nucl. Instruments Methods Phys. Res. Sect. B Beam Interact. with Mater. Atoms (2018).

[40] Q. Huang, H. Han, R. Liu, G. Lei, L. Yan, J. Zhou, Q. Huang, Acta Mater. 110 (2016) 1–7.

[41] C. Wang, T. Yang, J. Xiao, S. Liu, J. Xue, Q. Huang, J. Zhang, J. Wang, Y. Wang, J. Am. Ceram. Soc. 99 (2016) 1769–1777.

[42] M. Bugnet, V. Mauchamp, E. Oliviero, M. Jaouen, T. Cabioc'h, J. Nucl. Mater. 441 (2013) 133–137.

[43] V. Vishnyakov, J. Lu, P. Eklund, L. Hultman, J. Colligon, Vacuum 93 (2013) 56–59.

[44] G. Greaves, A.H. Mir, R.W. Harrison, M.A. Tunes, S.E. Donnelly, J.A. Hinks, Nucl. Instruments Methods Phys. Res. Sect. A Accel. Spectrometers, Detect. Assoc. Equip. 931 (2019) 37–43.

[45] R.E. Stoller, M.B. Toloczko, G.S. Was, A.G. Certain, S. Dwaraknath, F.A. Garner, Nucl. Instruments Methods Phys. Res. Sect. B Beam Interact. with Mater. Atoms 310

(2013) 75–80.

[46] A. Abdulkadhim, M. to Baben, T. Takahashi, V. Schnabel, M. Hans, C. Polzer, P. Polcik, J.M. Schneider, Surf. Coatings Technol. 206 (2011) 599–603.

[47] A.H. Mir, S. Peuget, I. Monnet, M. Toulemonde, S. Bouffard, C. Jegou, J. Nucl. Mater. 469 (2015) 244–250.

[48] D.V. Shtansky, P.V. Kiryukhantsev-Korneev, A.N. Sheveyko, B.N. Mavrin, C. Rojas, A. Fernandez, E.A. Levashov, Surf. Coatings Technol. 203 (2009) 3595–3609.

[49] J. Xiao, T. Yang, C. Wang, J. Xue, Y. Wang, J. Am. Ceram. Soc. 98 (2015) 1323–1331.

[50] Q. Huang, R. Liu, G. Lei, H. Huang, J. Li, S. He, D. Li, L. Yan, J. Zhou, Q. Huang, J. Nucl. Mater. 465 (2015) 640–647.

[51] S.J. Zinkle, J.T. Busby, Mater. Today 12 (2009) 12–19.

[52] S.J. Zinkle, G.S. Was, Acta Mater. 61 (2013) 735–758.

[53] G. Ackland, Science (80-.). 327 (2010) 1587.

[54] W.Z. Han, M.J. Demkowicz, E.G. Fu, Y.Q. Wang, A. Misra, Acta Mater. 60 (2012) 6341–6351.

[55] O. El-Atwani, A. Suslova, T.J. Novakowski, K. Hattar, M. Efe, S.S. Harilal, A. Hassanein, Mater. Charact. 99 (2015) 68–76.

[56] O. El-Atwani, J.E. Nathaniel, A.C. Leff, K. Hattar, M.L. Taheri, Sci. Rep. 7 (2017) 1836.

[57] L.F. He, M. Gupta, M.A. Kirk, J. Pakarinen, J. Gan, T.R. Allen, JOM 66 (2014) 2553–2561.

[58] J. Pakarinen, L. He, M. Gupta, J. Gan, A. Nelson, A. El-Azab, T.R. Allen, Nucl. Instruments Methods Phys. Res. Sect. B Beam Interact. with Mater. Atoms 319 (2014) 100–106.